Aalborg Universitet

AALBORG UNIVERSITY

Improved Extreme-Scenario Extraction Method For The Economic Dispatch Of Active Distribution Networks

Zhang, Yipu; Ai, Xiaomeng; Fang, Jiakun; Wen, Jinyu

Improved extreme-scenario extraction method for the economic dispatch of active distribution networks

Yipu Zhang[1], Xiaomeng Ai[1], Jiakun Fang[2], Jinyu Wen[1]

[1]*State Key Laboratory of Advanced Electromagnetic Engineering and Technology, Huazhong University of Science and Technology, Wuhan 430074, Hubei Province, People's Republic of China*
[2]*Department of Energy Technology, Aalborg University, Aalborg DK-9220, Denmark*
E-mail: yip.zhang@foxmail.com

Abstract: Optimisation techniques with good characterisation of the uncertainties in modern power system enable the system operators well trade-off between security and sustainability. This study proposes the extreme-scenario extraction-based robust optimisation method for the economic dispatch of active distribution network with renewables. The extreme scenarios are selected from the historical data using the improved minimum volume enclosing ellipsoid (MVEE) algorithm to guarantee the security of system operation while avoid frequently switching the transformer tap. It is theoretically proved that if the decision can be adaptive to the selected extreme scenarios, it can be robust to all the possible scenarios. Simulation results demonstrate that the proposed improved MVEE algorithm significantly reduces the number of scenarios, so that the computational burden is dramatically cut down. Additionally, compared to the existing robust optimisation approach, the proposed method is less conservative for the smaller size of the uncertainty set.

1 Introduction

In recent years, policy inventiveness and public awareness on the fossil fuel depletion promote rapidly development and increasingly deployment of renewable power generations. Besides the centralised wind farms or photovoltaic (PV) plants, renewable distributed generations (DGs) grow fast. According to the data from the National Energy Administration, as of the end of 2015, China's total installed capacity of PV power generation reached 43.18 GW, which made China become the world's largest country with PV power generation capacity [1]. However, the uncertainties of the renewables challenge the system operation [2, 3]. Especially in the distribution network, the voltage fluctuation threatens the secure operation of both the system and facilities.

Meanwhile, the reactive regulation devices in the distribution network such as switching capacitors and transformer tap changers cannot response fast enough to the constantly varying output of the DGs [4]. Therefore, how to effectively decide the status of such inflexible devices while fully use the flexibility resources in the system to well balance the security, economy, and sustainability becomes an urgent problem to be solved.

Traditionally, the reactive power optimisation in the distribution systems can be formulated as a mixed-integer non-linear programming problem, which can be solved by meta-heuristic algorithm [5–7] or the interior point method [8]. In [9], the non-convex non-linear has been converted to the second-order cone programming via the phase angle relaxation and conic relaxation. Compared to the meta-heuristic algorithms and the traditional interior point method, this relaxation can help to obtain the global optimal solution. Also based on the conic relaxation, Zheng *et al.* [10] propose an entirely distributed second-order cone programming solver based on the alternating direction method of multipliers algorithm. Lin *et al.* [11] presented a decentralised reactive power optimisation method based on the generalised Benders decomposition and the

second-order cone programming. However, none of the above studies involves the uncertainties of the DGs, which limits the practical application in real-world systems.

To encounter the uncertainties brought by the DGs, stochastic optimisation methods such as chance-constrained optimisation [12, 13] and robust optimisation techniques [14–18] can be used. Among the robust optimisation method, the uncertainty set is to describe the robust region which the optimal decision should be adaptive to. Constructing a proper uncertainty set plays an important role [19]. Large uncertainty set leads to conservative decisions. However, if the uncertainty set is too small, the system security cannot be guaranteed. Conventional robust optimisation uses the cubic set to describe the uncertainty without considering the correlations between the outputs of multiple renewable sources. For example, in [18], a two-stage robust reactive power optimisation in active distribution networks is proposed to determine the status of the reactive power compensation devices. Also, the model is solved effectively using the column-and-constraint generation algorithm. To reduce the conservativeness, ellipsoidal sets instead of the polyhedral set are defined [19] using the minimum volume enclosing ellipsoid (MVEE) algorithm, e.g. in [20, 21]. However, ellipsoidal sets still have two drawbacks: (i) the linear nature of the original model is changed because of the non-linear property of the uncertainty set; (ii) in the process of dealing with the ramping constraints, a series of new stochastic variables are introduced [20]. Therefore, the conservativeness of decision may increase with the number of stochastic variables. The extreme scenario method is also a way to deal with the random variables [22]. Also, the extraction of extreme scenario method is similar to the selection of uncertainty set in the robust optimisation. When the extreme scenarios are selected as the conventional cubic region, e.g. in [22], the number of the extreme scenarios increases exponentially with the dimension of the uncertain variables. In fact, the extreme-scenario extraction method can learn from the selection of the uncertainty set in the robust optimisation. Aiming at the

strong correlation of DGs in distribution network, the ellipsoidal sets based on the MVEE algorithm seem suitable.

So, in this paper, an extreme-scenario extraction algorithm applied to the conic programming is proposed. This method advances the existing work from two aspects: compared with chance-constrained optimisation and the existing extreme-scenario method, it significantly reduces the number of extracted extreme scenarios and the constraint satisfaction is guaranteed; compared with the robust optimisation, by considering the correlation of multiple DGs, the convex hull can be sized down so that better economics can be achieved. Meanwhile, the mathematical property of the original model will not be changed. Simulation results demonstrate the effectiveness of the proposed method.

2 Problem formulation

The economic dispatch (ED) in the conventional distribution systems with minimum active power loss as objective can be formulated as a quadratic programming [18]. Its generalised form can be written as

$$\min q(\boldsymbol{x}, \boldsymbol{y})$$
$$\text{s.t. } f(\boldsymbol{x}, \boldsymbol{y}) = 0, \quad g(\boldsymbol{x}, \boldsymbol{y}) \leq 0 \tag{1}$$

where q is the objective function. f and g are the equality and inequality constraints, respectively. The variables can be divided into two categories: $\boldsymbol{x}$ denotes the real-time adjustable variables such as the output of diesel engines, and $\boldsymbol{y}$ denotes those variables which cannot be changed for several hours or even the whole day such as the switching capacitors and the transformer tap. The optimisation problem (1) can be reformulated to the mixed integer conic programming [18]. Further using the convex relaxation techniques such as big M-approach, it can be formulated as the convex optimisation with guaranteed global optimality.

2.1 Uncertainties and extreme-scenario method

The increasingly deployed renewables have brought uncertainties to the modern distribution systems and challenged the system operation. When the uncertainties of DGs are considered, the deterministic optimisation (1) becomes stochastic

$$\min q(\boldsymbol{\xi}, \boldsymbol{x}, \boldsymbol{y})$$
$$\text{s.t. } f(\boldsymbol{\xi}, \boldsymbol{x}, \boldsymbol{y}) = 0, \quad g(\boldsymbol{\xi}, \boldsymbol{x}, \boldsymbol{y}) \leq 0 \tag{2}$$

where the new vector $\boldsymbol{\xi} \in \boldsymbol{R}^{n \times 1}$ consisting of the stochastic variables is introduced. n is the number of stochastic variables. In this work, possible instances of $\boldsymbol{\xi}$ are covered by historical operation data, denoted as $\boldsymbol{\xi}_{h,i} \in \boldsymbol{R}^{n \times 1}$. Extracted from the historical operation data, extreme scenarios $\boldsymbol{\xi}_{e,i} \in \boldsymbol{R}^{n \times 1}$ are selected. The number of the historical scenarios and the extreme scenarios are N_h and N_e, respectively.

With the extreme scenarios $\boldsymbol{\xi}_{e,i} \in \boldsymbol{R}^{n \times 1}$ selected, a two-stage optimisation is set up. The decision process is divided into two stages: at the first stage, the non-adjustable variables $\boldsymbol{y}$ are determined which will not change with the output of the DGs and constantly varying demands; the second stage determines the flexible adjustable variables $\boldsymbol{x}$ for those flexible sources with given $\boldsymbol{y}$. According to the extreme-scenario method, the stochastic optimisation becomes:

$$\min \sum_i q(\boldsymbol{\xi}_{e,i}, \boldsymbol{x}_{e,i}, \boldsymbol{y})$$
$$\text{s.t. } \begin{cases} f(\boldsymbol{\xi}_{e,1}, \boldsymbol{x}_{e,1}, \boldsymbol{y}) = 0, g(\boldsymbol{\xi}_{e,1}, \boldsymbol{x}_{e,1}, \boldsymbol{y}) \leq 0 \\ f(\boldsymbol{\xi}_{e,2}, \boldsymbol{x}_{e,2}, \boldsymbol{y}) = 0, g(\boldsymbol{\xi}_{e,2}, \boldsymbol{x}_{e,2}, \boldsymbol{y}) \leq 0 \\ \cdots \end{cases} \tag{3}$$

where in each line $\boldsymbol{\xi}_{e,i}$ denotes the ith extreme scenario; $\boldsymbol{x}_{e,i}$ denotes the adjustable variables for each scenario; the non-adjustable variable $\boldsymbol{y}$ remains the same for all the scenarios.

2.2 Extreme-scenario extraction

From the previous section, it can be seen that robust decision of the two-stage optimisation is highly dependent on the extraction of extreme scenario. On the one hand, the number of extreme scenarios affects the computational efficiency of the optimisation algorithm. On the other hand, the conservativeness of the decision is determined by the robust region. Conventional extreme scenario methods such as [22] tends to use the cubic uncertainty sets to cover all the possible instances of stochastic variable $\boldsymbol{\xi}$ due to the mathematical simplicity of dual conversion and same expression as the constraints of the traditional two-stage robust optimisation. In this work, the robust region is selected using another convex hull instead of cubic uncertainty sets. As long as all the possible instances are covered by the convex hull, the final decision can reach the same robustness level as the conventional robust optimisation with cubic uncertainty sets. Besides, the correlation between the stochastic variables is remained, which helps to reduce both the conservativeness and computational burden.

Next, in this section, the applicability of the extreme scenario-based two-stage optimisation is theoretically proved. Selecting the extreme scenarios as the vertexes of cubic set can be depicted in Fig. 1.

Theorem 1: If the decision variables $\boldsymbol{x}_{e,1}, \ldots, \boldsymbol{x}_{e,N_e}$ and $\boldsymbol{y}$ are adaptive to all the N_e extreme scenarios $\boldsymbol{\xi}_{e,1}, \ldots, \boldsymbol{\xi}_{e,N_e}$, it can ensure the existence of $\boldsymbol{x}_{h,i}$ and $\boldsymbol{y}$ in any historical scenario $\boldsymbol{\xi}_{h,i}$.

Proof: For the model suggested in this paper, f and part of g (denoted as g_1) are linear functions

$$\begin{cases} f(\boldsymbol{\xi}, \boldsymbol{x}, \boldsymbol{y}) = A_1 \boldsymbol{\xi} + B_1 \boldsymbol{x} + C_1 \boldsymbol{y} = 0 \\ g_1(\boldsymbol{\xi}, \boldsymbol{x}, \boldsymbol{y}) = A_2 \boldsymbol{\xi} + B_2 \boldsymbol{x} + C_2 \boldsymbol{y} \leq 0 \end{cases} \tag{4}$$

and the quadratic inequality g_2 is a convex function with adjustable variables $\boldsymbol{x}$ only. Assume $\boldsymbol{x} \in \boldsymbol{R}^{N+1 \times 1}$, its generalised form can be written as

$$g_2(\boldsymbol{x}) = \sqrt{\sum_{i=1}^{N} x_i^2} - x_{N+1} \leq 0 \tag{5}$$

Since the feasible region bounded by the extreme scenarios is a convex set, which is shown in Fig. 1, for any historical scenario $\boldsymbol{\xi}_{h,i}$, there is a set of positive real numbers $p_1, \ldots, p_{N_e}$ satisfying
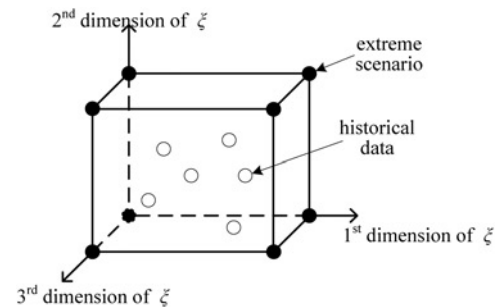

Fig. 1 *Example of extreme scenario*

$\sum_{j=1}^{N_e} p_j = 1$ and $\boldsymbol{\xi}_{h,i} = \sum_{j=1}^{N_e} p_j \times \boldsymbol{\xi}_{e,j}$. Apply the positive real numbers to the constraints in (4):

$$\begin{cases} p_1 g(\boldsymbol{\xi}_{e,1}, \boldsymbol{x}_{e,1}, \boldsymbol{y}) \le 0, & p_1 f(\boldsymbol{\xi}_{e,1}, \boldsymbol{x}_{e,1}, \boldsymbol{y}) = 0 \\ \quad\quad\quad\quad\vdots & \\ p_{N_e} g(\boldsymbol{\xi}_{e,N_e}, \boldsymbol{x}_{e,N_e}, \boldsymbol{y}) \le 0, & p_{N_e} f(\boldsymbol{\xi}_{e,N_e}, \boldsymbol{x}_{e,N_e}, \boldsymbol{y}) = 0 \end{cases} \quad (6)$$

Summarising f and g_1, (7) can be obtained

$$\begin{aligned} \sum_{j=1}^{N_e} p_j g_1(\boldsymbol{\xi}_{e,j}, \boldsymbol{x}_{e,j}, \boldsymbol{y}) &= g_1\left(\sum_{j=1}^{N_e} p_j \boldsymbol{\xi}_{e,j}, \sum_{j=1}^{N_e} p_j \boldsymbol{x}_{e,j}, \boldsymbol{y} \right) \\ \sum_{j=1}^{N_e} p_j f(\boldsymbol{\xi}_{e,j}, \boldsymbol{x}_{e,j}, \boldsymbol{y}) &= f\left(\sum_{j=1}^{N_e} p_j \boldsymbol{\xi}_{e,j}, \sum_{j=1}^{N_e} p_j \boldsymbol{x}_{e,j}, \boldsymbol{y} \right) \end{aligned} \quad (7)$$

Also, for convex function g_2, using *Jensen's* inequality, (8) can be obtained

$$\sum_{j=1}^{N_e} p_j g_2(\boldsymbol{x}_{e,j}) \ge g_2\left(\sum_{j=1}^{N_e} p_j \boldsymbol{x}_{e,j} \right) \quad (8)$$

For the variables $\boldsymbol{x}$, since its feasible region is also a convex set, the point $\boldsymbol{x}_{h,i} = \sum_{j=1}^{N_e} p_j \times \boldsymbol{x}_{e,j}$ is also inside the feasible region which means that the solution $\boldsymbol{x}_{h,i}$ and $\boldsymbol{y}$ for the scenario $\boldsymbol{\omega}_{h,i}$ exists. This completes the proof.

Remarks: The cubic set is not the necessary conditions. The practicability of the extreme-scenario method can be proved as long as the set bounded by the extreme scenarios is a convex set generally and the historical scenarios are all inside the convex set.

From this theorem, the applicability of combining the extreme scenario method and second-order conic programming is proved theoretically. Besides, it can be seen that, as long as all the possible instances are covered by the convex hull, the final decision can reach the same robustness level as the conventional robust optimisation with cubic uncertainty sets.

3 Improved MVEE algorithm for extreme-scenario extraction

After the proof of the applicability to combine the extreme scenario methods and the quadratic programming, this section introduces how the extreme scenarios can be selected according to the past experiences of system operation so that all the possibilities can be covered with very limited but critical scenarios. Take a three-dimensional $\boldsymbol{\xi}$ in Fig. 1, for example, it is intuitive to construct a cube containing all the historical operation conditions. However, using the cubic region to cover all the historical scenarios has two major drawbacks.

First, high-dimensional cubes have too many vertices. Also, the number of the extreme scenarios increases exponentially with the dimension of the uncertain variables, e.g. if the dimension of the uncertain variables $\boldsymbol{\xi}$ is n, the number of extreme scenarios is 2^n.

Additionally, the shape of the cubic region is too simple to characterise the spatial and time correlation of the DGs. Therefore, the improved MVEE algorithm is used in this paper to extract the extreme scenarios.

3.1 Improved MVEE algorithm

The basic idea of the improved MVEE algorithm is to use an ellipsoid instead of a cubic set to cover all the possible instances of $\boldsymbol{\xi}$. Then the vertices of the ellipsoid are selected as the extreme scenarios. Compared to the cubic set with 2^n vertices, the vertex number of the ellipsoid is proportional to the dimensions of $\boldsymbol{\xi}$, i.e. for

n-dimensional $\boldsymbol{\xi}$, the number of extracted extreme scenarios can be reduced from 2^n to $2 \times n$.

A full-dimensional ellipsoid E represented by a symmetric positive definite matrix $\boldsymbol{Q} \in \boldsymbol{R}^{n \times n}$ and a centre $\boldsymbol{c} = [c_1, \ldots, c_n]^T$ can be mathematically defined as:

$$E(\boldsymbol{Q}, \boldsymbol{c}) = \{\boldsymbol{\xi} \in \boldsymbol{R}^n | (\boldsymbol{\xi} - \boldsymbol{c})^T \boldsymbol{Q} (\boldsymbol{\xi} - \boldsymbol{c}) \le 1\} \quad (9)$$

Since the ellipsoid can be linearly transformed from a sphere in $\boldsymbol{R}^n$ space, the volume of E can be calculated by the volume of the unit sphere ρ_n times the transformation

$$\text{Vol}(E) = \rho_n \det \boldsymbol{Q}^{-1/2} \quad (10)$$

To obtain the ellipsoid with minimum volume is to calculate $\boldsymbol{Q}$ and $\boldsymbol{c}$ by solving the following optimisation problem

$$\begin{aligned} &\min \rho_n \det \boldsymbol{Q}^{-(1/2)} \\ &\text{s.t.} \quad (\boldsymbol{\xi}_{h,1} - \boldsymbol{c})^T \boldsymbol{Q}(\boldsymbol{\xi}_{h,1} - \boldsymbol{c}) \le 1 \\ &\quad\quad (\boldsymbol{\xi}_{h,2} - \boldsymbol{c})^T \boldsymbol{Q}(\boldsymbol{\xi}_{h,2} - \boldsymbol{c}) \le 1 \\ &\quad\quad \cdots \end{aligned} \quad (11)$$

where all the historical scenarios $\boldsymbol{\xi}_{h,i}$ are taken into account. The optimisation (11) is a quadratic programming, which can be solved with existing algorithm efficiently [20].

3.2 Vertices of the ellipsoid

After the matrix $\boldsymbol{Q}$ and vector $\boldsymbol{c}$ are obtained, the vertices of the ellipsoid are selected as extreme scenarios.

To obtain the mathematical express of the vertices, the original ellipsoid E is transformed into an axial ellipsoid E' according to orthogonal decomposition:

$$E'(\boldsymbol{D}) = \{\boldsymbol{\xi}' \in \boldsymbol{R}^n | \boldsymbol{\xi}'^T \boldsymbol{D} \boldsymbol{\xi}' \le 1\} \quad (12)$$

In (12), the new stochastic vector $\boldsymbol{\xi}'$ and the new matrix $\boldsymbol{D}$ satisfy:

$$\boldsymbol{\xi}' = \boldsymbol{P} \times (\boldsymbol{\xi} - \boldsymbol{c}) \quad (13)$$

$$\boldsymbol{D} = \text{diag}(\lambda_1, \lambda_2, \ldots, \lambda_n) \quad (14)$$

$$\boldsymbol{Q} = \boldsymbol{P}^T \boldsymbol{D} \boldsymbol{P} = \boldsymbol{P}^{-1} \boldsymbol{D} \boldsymbol{P} \quad (15)$$

Here, the $\boldsymbol{P}$ is the orthogonal matrix used for orthogonal decomposition (15) and $\boldsymbol{D}$ is a diagonal matrix consists of eigenvalues of positive definite matrix $\boldsymbol{Q}$. For the axial ellipsoid E', the matrix which the column vectors consist of the $2 \times n$ vertices coordinates can be expressed as:

$$V' = \pm \text{diag}(\lambda_1^{-1/2}, \lambda_2^{-1/2}, \ldots, \lambda_n^{-1/2}) \in \boldsymbol{R}^{n \times 2n} \quad (16)$$

As for the extreme scenarios, which can be denoted as the vertices of the original ellipsoid, according to the inverse transformation of (13), the mathematical expression of the vertices of E can get

$$V = \begin{pmatrix} c_1 & \cdots & c_1 \\ \vdots & \ddots & \vdots \\ c_n & \cdots & c_n \end{pmatrix}_{n \times 2n} + \boldsymbol{P}^{-1} V' \quad (17)$$

4 Numerical results

4.1 System description

To validate the effectiveness of the proposed algorithm, a 69-bus distribution network is used as the test system. IBM ILOG
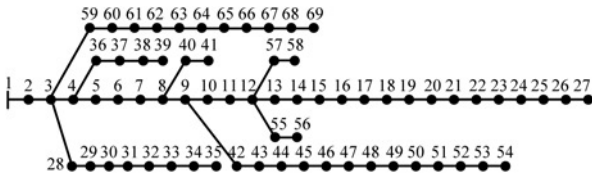
Fig. 2 *System topology*

CPLEX is used as the MIQCP solver. The parameters of the 69-bus radial system can be found in [18].

The total load is 5.0484 MW + 2.6817 MVar, and three voltage levels are 35, 10.5, and 0.4 kV. The topology of the system is shown in Fig. 2. Branches 14–15, 28–29, 59–60, 36–37, and 42–43 are 35–10.5 kV transformers equipped with tap changers, denoted as T1–T5. Branch 18–19 is a 10.5–0.4 kV transformer with tap changer, denoted as T6. The minimum step change of tap ratio is set to 0.025, and the regulation range is set to [0.95, 1.05] for all the transformers. Two PV systems and one wind generator are connected to bus 25, bus 33, and bus 16, respectively. The output data is obtained from the historical data of DGs in a certain region of Australia [23]. The tap ratios belong to the non-adjustable variables at first-stage optimisation, while the active and reactive power from bus 1 are adjustable variables at second-stage optimisation.

4.2 Operational cost and security

With given system topology and historical data, the optimisation problem is solved with the proposed method. The tap ratios of the transformers are shown in Table 1.

After the first-stage variables are determined, historical data is randomly sampled to verify whether the second-stage variables can adapt to the fluctuations of the renewable generations, which is shown in Fig. 3. The green dots indicate the historical operating conditions to which the first-stage optimisation results are adaptive. It can be seen that the robustness of the first-stage decision is validated.

This subsection also compares the extreme scenarios extraction algorithms using cubic set and the method proposed in this paper. Take the two-dimensional case for example. The region obtained by (17) covers less area than the cube, as shown in Fig. 4. This means that in the cubic region, a lot of non-existence scenarios are included which the system has no need to be robust to. The improved MVEE algorithm, by considering the correlation of output power of DGs, reduces the system operational cost while maintains the security.

Table 1 Optimal values of the first-stage variable

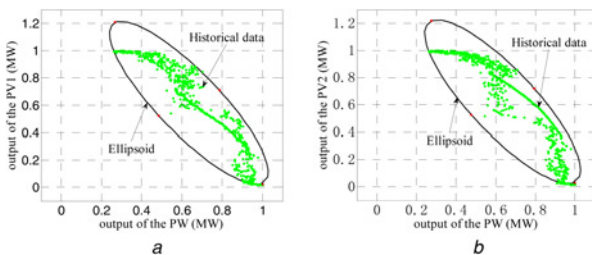| T1	T2	T3	T4	T5	T6
1.05	0.975	1	1	1.05	1

Fig. 3 *Projection of the historical data in the two-dimensional surface*
a Projection of the historical data in 'PW-PV1' surface
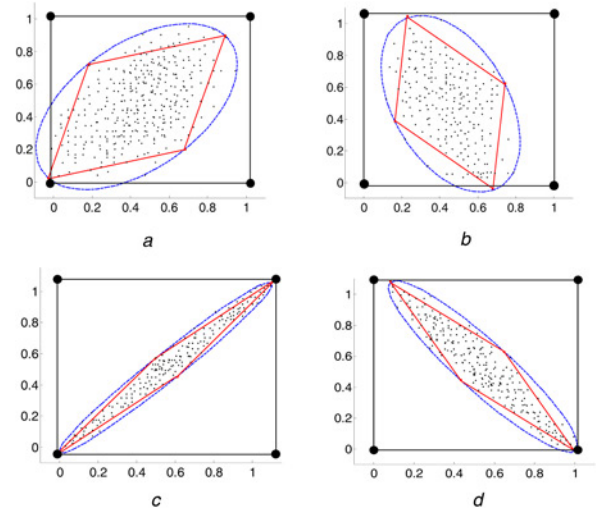b Projection of the historical data in 'PW-PV2' surface

Fig. 4 *Space described by the improved MVEE and cubic region with different correlation*
a Space with a weak positive correlation
b Space with a weak negative correlation
c Space with a strong positive correlation
d Space with a strong negative correlation

From the power system point of view, larger area in Fig. 4 indicates that more compensation devices must be turned on so that the optimality for the first-stage optimisation exists. In the following test simulation, we gradually decrease the reactive power capacity in the distribution system. The test results are shown in Table 2. When the pre-set reactive capacity is <3 MVar, the optimisation of system operation is no longer feasible because the cubic region algorithm considers some needless scenarios.

4.3 Computational efficiency and effectiveness

In the studied system, the major uncertainties come from the DGs. The relationship between the number of the extracted extreme scenarios and the number of the DGs with the proposed method is proportional. However, for the cubic region method, it is an exponential relationship. The computational time is compared in Table 3.

Table 2 Status of the optimisation solution with the reactive power configuration changing. √ denotes the optimisation has a feasible solution and × denotes not

Reactive power configuration, MVar	Improved MVEE	Cubic set
3.20	√	√
2.96	√	×
2.85	√	×
2.80	×	×

Table 3 Calculation time with the number of DGs changing

Number of DGs	Improved MVEE		Cubic set	
	Number of the extreme scenarios	Calculation time, s	Number of the extreme scenarios	Calculation time, s
2	4	2.03	4	2.94 s
3	6	7.8	8	13.5 s
4	8	11.45	16	24.1 s
5	10	13.87	32	72.7 s
6	12	15.94	64	—
7	14	18.63	128	—

Table 4 Testing of the conic relaxation

Number of DGs	First stage	Second stage
3	0.0002	3.7726×10^{-4}
4	0.0005	1.2853×10^{-4}
5	0.0002	2.6854×10^{-4}
6	0.0002	3.6301×10^{-4}
7	0.0004	1.9494×10^{-4}

It can be seen that for the proposed improved MVEE algorithm, the number of extracted extreme scenarios increases much slower than the cubic set algorithm proposed in [22]. Also hence less computational time is needed. When the number of DGs exceeds five, the cubic set algorithm fails to reach the optimality in the reasonable time. So only the proposed algorithm can be applied to a large-scale distribution system with quite a lot of renewable DGs.

In the conic relaxation of the optimisation, the equality constraints (18) are transformed to the inequality constraints (19) according to [9]

$$P_{ij}^2 + Q_{ij}^2 = I_{ij}^2 \cdot U_i^2 \qquad (18)$$

$$P_{ij}^2 + Q_{ij}^2 \leq I_{ij}^2 \cdot U_i^2 \qquad (19)$$

To validate the equivalency of the problems before and after transformation, the error is defined as (20) to see if the equality constraints can be met:

$$\Delta = \left| P_{ij}^2 + Q_{ij}^2 - I_{ij}^2 \cdot U_i^2 \right| \qquad (20)$$

From the physical system point of view, (20) indicates the power balance. For the non-adjustable variables determined at the first-stage optimisation, the error for all the extreme scenarios is summed. While for the adjustable variables at the second stage, errors for all the possible scenarios are summed. The test results are shown in Table 4.

5 Conclusion

In this paper, the improved extreme-scenario extraction method for the ED of active distribution system is proposed. It is theoretically proved that the applicability of combining the extreme scenario method and second-order conic programming. Case studies show that the proposed algorithm well balances the robustness and economics of system operation by taking the correlations of the DGs into account. The proposed algorithm is superior to the cubic set-based algorithm with lower operation cost while without loss of security. In addition, the computational efficiency is significantly improved so that the proposed method is applicable to large distribution systems with lots of DGs.

6 Acknowledgments

7 References

[1] Liu P., Tan Z.: 'How to develop distributed generation in China: in the context of the reformation of electric power system', *Renew. Sustain. Energy Rev.*, 2016, **66**, (12), pp. 10–26

[2] Najy W.K.A., Zeineldin H.H., Woon W.L.: 'Optimal protection coordination for microgrids with grid-connected and islanded capability', *IEEE Trans. Ind. Electron.*, 2013, **60**, (4), pp. 1668–1677

[3] Atanasovski M., Taleski R.: 'Energy summation method for loss allocation in radial distribution networks with DG', *IEEE Trans. Power Syst.*, 2012, **27**, (3), pp. 1433–1440

[4] Antoniadou-Plytaria K.E., Kouveliotis-Lysikatos I.N., Georgilakis P. S., ET AL.: 'Distributed and decentralized voltage control of smart distribution networks: models, methods, and future research', *IEEE Trans. Smart Grid*, 2017, **8**, (6), pp. 2999–3008

[5] Lee K.Y., Yang F.F.: 'Optimal reactive power planning using evolutionary algorithms: a comparative study for evolutionary programming, evolutionary strategy, genetic algorithm, and linear programming', *IEEE Trans. Power Syst.*, 1998, **13**, (1), pp. 101–108

[6] Zhang W., Li F., Tolbert L.M.: 'Review of reactive power planning: objectives, constraints, and algorithms', *IEEE Trans. Power Syst.*, 2007, **22**, (4), pp. 2177–2186

[7] Wang Y., Li F., Wan Q., ET AL.: 'Reactive power planning based on fuzzy clustering, gray code, and simulated annealing', *IEEE Trans. Power Syst.*, 2011, **26**, (4), pp. 2246–2255

[8] Liu M.B., Tso S.K., Cheng Y.: 'An extended nonlinear primal-dual interior-point algorithm for reactive-power optimization of large-scale power systems with discrete control variables', *IEEE Trans. Power Syst.*, 2002, **17**, (4), pp. 982–991

[9] Farivar M., Low S.H.: 'Branch flow model: relaxations and convexification – part I', *IEEE Trans. Power Syst.*, 2013, **28**, (3), pp. 2554–2564

[10] Zheng W., Wu W., Zhang B., ET AL.: 'A fully distributed reactive power optimization and control method for active distribution networks', *IEEE Trans. Smart Grid*, 2016, **7**, (2), pp. 1021–1033

[11] Lin C., Wu W., Zhang B., ET AL.: 'Decentralized reactive power optimization method for transmission and distribution networks accommodating large-scale DG integration', *IEEE Trans. Sustain. Energy*, 2017, **8**, (1), pp. 363–373

[12] Kargarian A., Fu Y., Wu H.: 'Chance-constrained system of systems based operation of power systems', *IEEE Trans. Power Syst.*, 2016, **31**, (5), pp. 3404–3413

[13] Cao Y., Tan Y., Li C., ET AL.: 'Chance-constrained optimization-Based unbalanced optimal power flow for radial distribution networks', *IEEE Trans. Power Deliv.*, 2013, **28**, (3), pp. 1855–1864

[14] Jabr R.A.: 'Robust transmission network expansion planning with uncertain renewable generation and loads', *IEEE Trans. Power Syst.*, 2013, **28**, (4), pp. 4558–4567

[15] Jiang R., Wang J., Zhang M., ET AL.: 'Two-stage minimax regret robust unit commitment', *IEEE Trans. Power Syst.*, 2013, **28**, (3), pp. 2271–2282

[16] Li J., Wen J., Han X.: 'Low-carbon unit commitment with intensive wind power generation and carbon capture power plant', *J. Mod. Power Syst. Clean Energy*, 2015, **3**, (1), pp. 63–71

[17] Jiang R., Wang J., Guan Y.: 'Robust unit commitment with wind power and pumped storage hydro', *IEEE Trans. Power Syst.*, 2012, **27**, (2), pp. 800–810

[18] Ding T., Liu S., Yuan W., ET AL.: 'A two-stage robust reactive power optimization considering uncertain wind power integration in active distribution networks', *IEEE Trans. Sustain. Energy*, 2016, **7**, (1), pp. 301–311

[19] Guan Y., Wang J.: 'Uncertainty sets for robust unit commitment', *IEEE Trans. Power Syst.*, 2014, **29**, (3), pp. 1439–1440

[20] Ding T., Lv J., Bo R., ET AL.: 'Lift-and-project MVEE based convex hull for robust SCED with wind power integration using historical data-driven modeling approach', *Renew. Energy*, 2016, **92**, pp. 415–427

[21] Wu W., Wang K., Li G.: 'Affinely adjustable robust unit commitment considering the spatiotemporal correlation of wind power', *Proc. CSEE* (in Chinese), 2017, **37**, (14), pp. 4089–4097

[22] Ye R., Chen H., Wang G., ET AL.: 'A mixed integer programming method for security-constrained unit commitment with multiple wind farms', *Autom. Electr. Power Syst.*, 2010, **34**, (5), pp. 29–33 (in Chinese)

[23] http://solar.uq.edu.au/user/reportPower.php